Advanced Agent Identification With Fluctuation-Enhanced Sensing

Chiman Kwan, *Senior Member, IEEE*, Gabor Schmera, Janusz M. Smulko, *Member, IEEE*, Laszlo B. Kish, Peter Heszler, and Claes-Göran Granqvist

Invited Paper

***Abstract*—Conventional agent sensing methods normally use the steady state sensor values for agent classification. Many sensing elements (Hines *et al.*, 1999; Ryan *et al.*, 2004; Young *et al.*, 2003; Qian *et al.*, 2004; Qian *et al.*, 2006; Carmel *et al.*, 2003) are needed in order to correctly classify multiple agents in mixtures. Fluctuation-enhanced sensing (FES) looks beyond the steady-state values and extracts agent information from spectra and bispectra. As a result, it is possible to use a single sensor to perform multiple agent classification. This paper summarizes the application of some advanced algorithms that can classify and estimate concentrations of different chemical agents. Our tool involves two steps. First, spectral and bispectral features will be extracted from the sensor signals. The features contain unique agent characteristics. Second, the features are fed into a hyperspectral signal processing algorithm for agent classification and concentration estimation. The basic idea here is to use the spectral/bispectral shape information to perform agent classification. Extensive simulations have been performed by using simulated nanosensor data, as well as actual experimental data using commercial sensor (Taguchi). It was observed that our algorithms are able to accurately classify different agents, and also can estimate the concentration of the agents. Bispectra contain more information than spectra at the expense of high-computational costs. Specific nanostructured sensor model data yielded excellent performance because the agent responses are additive with this type of sensor. Moreover, for measured conventional sensor outputs, our algorithms also showed reasonable performance in terms of agent classification.**

***Index Terms*—Chemical agent, fluctuation-enhanced sensing (FES), identification.**

I. Introduction

DETECTION of chemical and biological agents is critical for military operations and civilian applications. In military applications, detection of chemical and biological agents will significantly reduce the number of casualties. In civilian applications, agent detection and classification will be extremely useful in homeland security (airport safety, federal buildings, courthouses, etc.) to prevent terrorist attacks.

It is well known that there are several limitations in the conventional agent detection systems. First, conventional approaches to agent detection focus on steady-state values and simply ignore the microfluctuations in the sensor [5]–[15]. In recent years, Kish and his collaborators [4], [16]–[21] have demonstrated that the fluctuations in the sensor contain characteristics of different agents and have several orders of higher sensitivity than that of the steady values of the sensors. Second, conventional methods need to tune to certain agents, which significantly limits the performance of detecting other agents. Third, in order to achieve certain sensitivity, a huge number of molecules have to be absorbed by the sensor, resulting in slow response. Fourth, conventional approaches normally require a large number of sensing elements [5]–[10] in the sensor and, hence, may be more susceptible to sensor failures.

In this paper, we propose a high-performance chemical and biological agent classification system, which will significantly improve the commercial-off-the-shelf (COTS) sensors and other future nanosensors.

Fig. 1 shows the architecture of the proposed FES-based system. An Invention Disclosure has been filed and a patent will be filed soon. There are several key components. First, a low-noise amplifier will be used to amplify the small fluctuations in the sensor signals. Many useful features will be extracted from the fluctuation signals. Second, the mean sensor outputs, the mean-square fluctuations, and high-order statistics (skewness and kurtosis) will be fed into a robust classifier known as support vector machine (SVM) for agent detection and classification. This method is efficient, does not have an overfitting problem, and has been proven to outperform multilayer perceptron neural network in many applications. Third, we propose to apply the latest results in hyperspectral signal processing to the power spectrum, bispectrum, and amplitude density functions. The particular hyperspectral technique is known as non-negativity constrained least square (NCLS) [1]. NCLS is efficient and can also estimate the concentration of component agents from a mixture based on spectral shape information of a mixture. Fourth, to further enhance the robustness of the overall system, a decision level fusion will be used to fuse the decisions from various classifiers. Finally, classified

Manuscript received August 14, 2007; revised December 31, 2007; accepted January 15, 2008. This work was supported in part by the U.S. Army Research Organization under Contract W911NF-07-C-0021.

C. Kwan is with Signal Processing, Inc., Rockville, MD 20850 USA (e-mail: chiman.kwan@ signalpro.net).

G. Schmera is with the Space and Naval Warfare Systems Center, San Diego, CA 92152 USA.

J. M. Smulko is with the Gdansk University of Technology, 80-952 Gdansk, Poland.

L. B. Kish is with the Texas A&M University, College Station, TX 77843 USA.

P. Heszler is with the Research Group on Laser Physics, Hungarian Academy of Sciences, University of Szeged, 6701 Szeged, Hungary.

C.-G. Granqvist is with the Uppsala University, 751 05 Uppsala, Sweden.

Color versions of one or more of the figures in this paper are available online at http://ieeexplore.ieee.org.

Digital Object Identifier 10.1109/JSEN.2008.923029

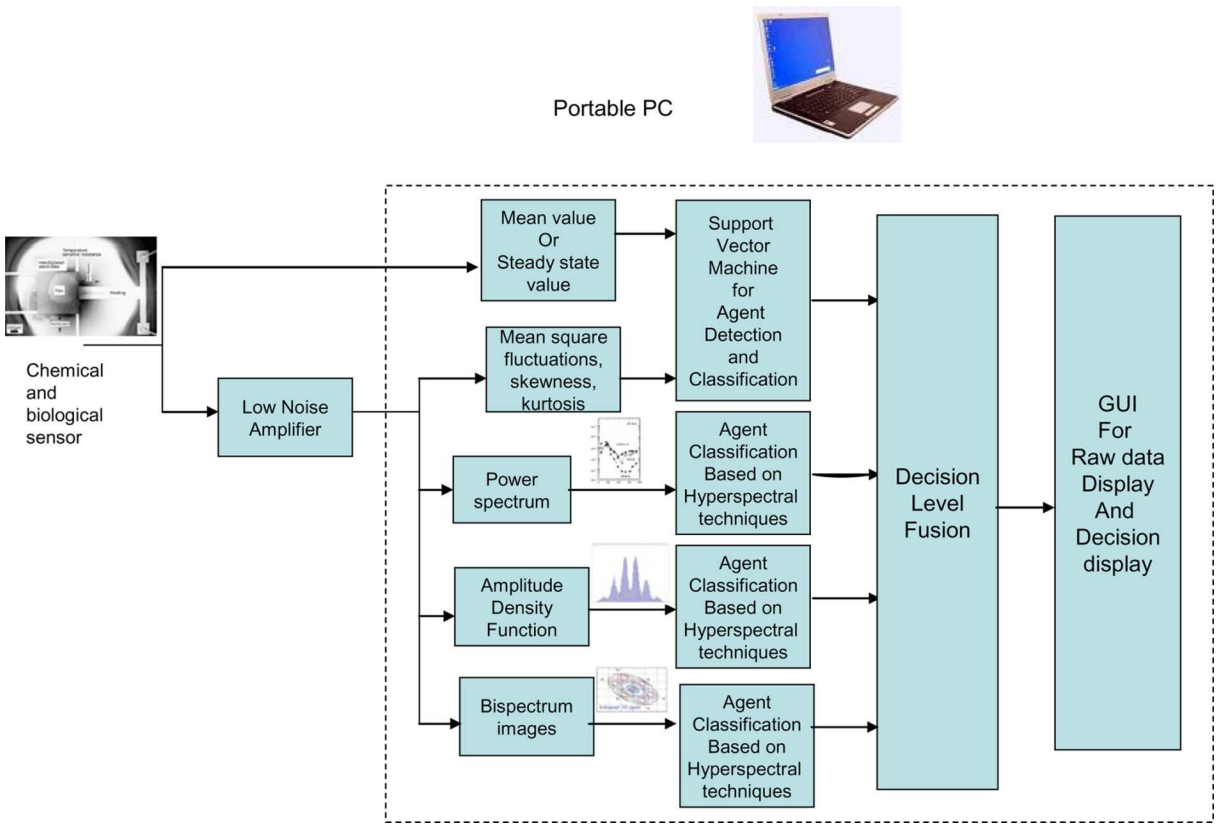

Fig. 1. FES-based architecture for high-performance chemical sensing.

agent names and raw data will be displayed on the monitor of a laptop.

Details of the technical components will be briefly described below. Our system offers the following significant advantages.

- High performance: Due to the use of fluctuation enhanced techniques.
- General: Can deal with chemical and biological agents.
- Accurate concentration estimation in addition to detection and classification.
- Utilization of both low-order and high-order statistics to yield accurate and robust agent classification. Low-order statistics include mean sensor value, power spectrum, mean-square fluctuations, and amplitude density functions. High-order statistics include skewness, kurtosis, and bispectrum images.
- Sensitive detection (low false alarm rate and high probability of detection) due to the use of advanced and proven processing algorithms (SVM, NCLS). Decision level fusion will be performed to generate even more accurate classifications.
- Real-time processing capability (high-throughput).
- Easy to visualize results (user friendly).

This paper is organized as follows. Section II reviews the components in the proposed FES framework. Section III presents some simulation studies using nanosensor data and conventional sensor data. Finally, conclusions will be given in Section IV.

II. Overview of the Algorithm Framework

A. Low- and High-Order Statistics

Suppose we have a data set with M sensors and a window length N for each sensor, the means and standard deviations of the data are, respectively, defined as

$$\bar{x}_i = \frac{\sum_{j=K+1}^{K+N} x_{ij}}{N}$$

$$\sigma_i = \sqrt{\frac{\sum_{j=K}^{K+N} (x_{ij} - \bar{x}_i)^2}{N}}$$

where x_{ij} is the jth data element of the ith sensor. It should be noted that we compute the means and standard deviations from data elements $K+1$ to $K+N$. This is to make sure that the means and standard deviations are in the steady-state.

In some situations, the gas-induced noise may have high-order statistical behaviors and the low-order statistical measures may not be effective in differentiating the different gases. Here, we use two high-order features: skewness and kurtosis. The skewness for a normal distribution is zero, and any symmetric data should have a skewness near zero. Negative values for the skewness indicate data that are skewed left and positive values for the skewness indicate data that are skewed right. Some measurements have a lower bound and are skewed right. For ex-

ample, in reliability studies, failure times cannot be negative. The standard normal distribution has a kurtosis of zero. Positive kurtosis indicates a "peaked" distribution and negative kurtosis indicates a "flat" distribution.

Suppose we have a data set with M sensors and a window length N for each sensor, the skewness and kurtosis of the data are, respectively, defined as

$$S_i = \frac{\sum_{j=K+1}^{N+K}(x_{ij}-\bar{x}_i)^3}{(N-1)\sigma_i^3}$$
$$Ku_i = \frac{\sum_{j=K+1}^{N+K}(x_{ij}-\bar{x}_i)^4}{(N-1)\sigma_i^4} - 3. \quad (1)$$

B. Power Spectrum

Given a time series, one usually applies fast-Fourier transform (FFT) to it and then takes the square of the coefficients to yield the energy spectrum. The above definition of energy spectral density requires that the Fourier transforms of the signals exist, that is, the signals are square-integrable or square-summable. An often more useful alternative is the **power spectral density** (PSD), which describes how the power of a signal or time series is distributed with frequency.

Since a signal with nonzero average power is not square integrable, the Fourier transforms do not exist in this case. The PSD is the Fourier transform of the autocorrelation function of the signal if the signal can be treated as a stationary random process.

C. Bispectrum

The second- and third-order cumulants $C_{2x}(k)$, $C_{3x}(k,l)$ of a zero-mean stationary process, $x(n)$, is defined in (2) and (3), respectively

$$C_{2x}(k) = E\{x^*(n)x(n+k)\} \quad (2)$$
$$C_{3x}(k,l) = E\{x^*(n)x(n+k)x(n+l)\} \quad (3)$$

where $C_{2x}(k)$ is the second-order cumulant and $C_{3x}(k,l)$ is the third-order cumulant. The second-order polyspectrum (also known as power spectrum), $S_{2x}(f)$, is expressed in (4) and the third-order polyspectrum, $S_{3x}(f_1,f_2)$, which is known as bispecrum, is expressed in (5)

$$S_{2x}(f) = \sum_{k=-\infty}^{\infty} C_{2x}(k)e^{-j2\pi fk} \quad (4)$$
$$S_{3x}(f_1,f_2) = \sum_{k=-\infty}^{\infty}\sum_{l=-\infty}^{\infty} C_{3x}(k,l)e^{-j2\pi f_1 k}e^{-j2\pi f_2 k}. \quad (5)$$

Suppose $x(n)$, $x(n)=\sum_k h(k)u(n-k)$, is a linear process where $u(n)$ is independent and identically distributed (iid) and $h(n)$ is the impulse response. Using these definitions, the second-order and third-order cumulants can also be mathematically expressed as

$$C_{2x}(k) = \gamma_{2u}\sum_n h^*(n)h(n+k) \quad (6)$$
$$C_{3x}(k,l) = \gamma_{3u}\sum_n h^*(n)h(n+k)h(n+l) \quad (7)$$

where $\gamma_{ku} = C_{ku}$. The power spectrum and bispectrum can be expressed using the frequency response information as

$$S_{2x}(f) = \gamma_{2u}|H(f)|^2 \quad (8)$$
$$S_{3x}(f_1,f_2) = \gamma_{3u}H(f_1)H(f_2)H^*(f_1+f_2) \quad (9)$$

where $H(f)$ is the frequency response. It can be seen from (8) and (9) that the power spectrum does not carry any information about the phase of $H(f)$, while if $u(n)$ is non-Gaussian, the phase information can be recovered with the bispectrum.

D. Hyperspectral Unmixing Algorithm

Suppose that there are p chemicals $\mathbf{t}_1,\mathbf{t}_2,\ldots,\mathbf{t}_p$. Let $\mathbf{m}_1,\mathbf{m}_2,\ldots,\mathbf{m}_p$ be their corresponding spectral signatures. Suppose L is the number of spectral bands in $\mathbf{m}_j$, where $1 \le j \le p$. Let $\mathbf{r}$ denote a linear mixture of $\mathbf{m}_1,\mathbf{m}_2,\ldots,\mathbf{m}_p$ with appropriate abundance fractions specified by $\alpha_1,\alpha_2,\ldots,\alpha_p$, which can be denoted by a $L\times 1$ column vector. Let $\mathbf{M}$ denote the $L\times p$ target spectral signature matrix, depicted by $[\mathbf{m}_1,\mathbf{m}_2,\ldots,\mathbf{m}_p]$. Let $\boldsymbol{\alpha} = [\alpha_1,\alpha_2,\ldots,\alpha_p]^T$ be a $p\times 1$ abundance column vector associated with $\mathbf{r}$, where α_j denotes the abundance fraction of $\mathbf{m}_j$ that is present in the mixture $\mathbf{r}$. The spectral signature of the mixture, $\mathbf{r}$, can be modeled in a linear regression form as

$$\mathbf{r} = \mathbf{M}\boldsymbol{\alpha} + \mathbf{n} \quad (10)$$

where $\mathbf{n}$ is the noise or can be interpreted as a measurement error or a model error.

The non-negative constrained least square (NCLS) is an algorithm that can be used to accurately estimate α_j. The magnitude of α_j will indicate the concentration of chemical j. Hence, the recognition process kills two birds will one stone. We can simultaneously estimate the abundance as well as identify the chemicals. The algorithm is quite complicated. Details can be found in our paper [1].

It should be noted that we also have implemented some other hyperspectral signal processing tools, including orthogonal subspace projection (OSP), spectral angle mapper, etc., in our real-time C-based product.

E. Support Vector Machine for Classification

After the features have been extracted, we can feed the features into the SVM for classification. The following paragraphs are summarized from [2]. The geometrical interpretation of SVM is that the algorithm searches for the optimal separating surface, i.e., the hyperplane that is, in a sense, equidistant from the two classes assuming a two-class problem.

The advantages of SVM include [2] the following.

- It is a quadratic learning algorithm with no local optima.
- Statistical theory gives bounds on the expected performance of a support machine.
- SVM can be applicable to multiclass classification applications.
- There is no overtraining problem as compared with conventional learning classifiers such as neural net or fuzzy logic. This is because only the support vectors are needed for classification.

F. Dempster Shafer Fusion to Yield Robust Decisions

Dempster Shafer (DS) fusion [22] is a well-known technique in robust decision fusion. This procedure requires a three-dimensional $N \times C \times M$ matrix which contains the class probability values, where N is the number of classifiers (or classification outputs), C is the number of classes (or gases), and M is the number of samples (or tests).

For each test, a matrix of decisions is generated. The $N \times C$ matrix is defined as

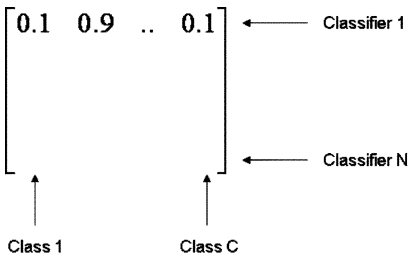

To generate a classification decision for a given test, the sum of the products of every pair in each column of the above matrix is added to yield a combined decision for a class. In other words, for column i of the above matrix, if the elements in that column are $d_{i1}, d_{i2}, \ldots, d_{iN}$, then the combined classification for class i will be

$$\sum_{k=1}^{N} \sum_{j=k+1}^{N} d_{ik} d_{ij}.$$

The decisions from all the columns will be combined into a $C \times 1$ vector. The class label of the maximum value in the $C \times 1$ vector will be the fused result. Similarly, we can generate the fused decisions for all the other tests.

III. Main Results

A. Nanosensor Analysis

The Space and Naval Warfare Systems Center has developed a simulation software package that can simulate the behavior of nanosensors. The basic idea is to use a one-dimensional random walk model to simulate the behavior of the nanosensor. The geometry is assumed to be symmetrical about the origin with reflecting boundaries at -10 and $+10$; the "sweetspot" is located between -1 and $+1$. We assumed to have N molecules of k different types on the sensing surface. Each molecule type has a different diffusion constant. Let N be the total number of molecules with $N = n_1 + n_2 + \cdots + n_k$, where n_i is the number of molecules of the ith type. The initial positions of the molecules were chosen randomly between the boundaries. Each of the N molecules performed a random walk on the sensor surface; we assumed no interaction between the molecules.

The output signal u of the sensor is a weighted sum of the number of molecules residing in the "sweet spot"

$$u = c_1\nu_1 + c_2\nu_2 + \cdots + c_n\nu_n$$

where c_i is the contribution of a single molecule of the ith type to the output and ν_i is the number of molecules of the ith type that currently reside in the "sweetspot."

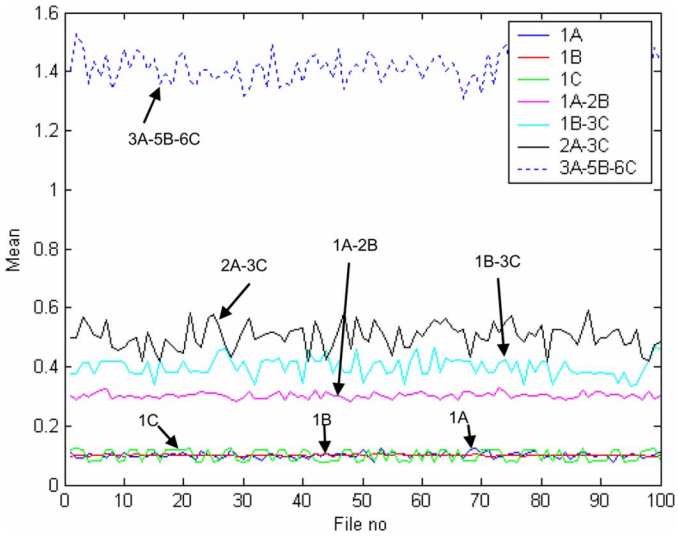

Fig. 2. Mean values of data with different number of molecules.

We performed many simulations and generated the following seven data sets.

- Cases: 1A, 1B, 1C, 1A-2B, 1B-3C, 2A-3C, 3A-5B-6C. Case 1A contains sensor behavior in the presence of one molecule of type A. Cases 1B-3C contains sensor behavior in the presence of 1 molecule B and 3 molecules of C. The other cases can be similarly understood.
- Each case consists of 100 files.
- Each file consists of 2^20 (1,048,576 data points).

It should be noted that it is impossible to use mean values to distinguish different gases. Fig. 2 shows the mean value plots of data with different number of molecules. We could not generate meaningful outputs of ROC by using mean values. For example, the data with 1A, 1B, and 1C all have the same mean values. It is, therefore, impossible to distinguish the molecule types based on means. However, by using spectral and bispectral shapes, we can indeed differentiate different types of molecules.

Here, ROC curve analysis is applied to compare the performances of using FFT and bispectrum signatures. The formulation for applying ROC analysis in this work is established as follows.

Suppose a measurement has been conducted. There are two hypotheses regarding the existence of gas molecule type (i) in the measurement.

1) There is "type i gas molecule" in the measurement.
2) There is "no type i gas molecule" in the measurement.

A scalar threshold range is defined between 0 and 1 with an incremental value of 0.001. Suppose the scalar threshold within this range is denoted by the notation *threshold*. Similar to the previously applied error-based metric, two conditions are considered. The first condition is where the actual abundances are *not equal to zero* and the second condition is where actual abundances are *equal to zero*. The first condition thus corresponds to the computation of the probability of detection rate (PD) and the second condition corresponds to the computation of the false alarm rate (FA). In the computation of the probability of detection (PD), suppose h denotes the number of counts for hits (it should be noted that the term *hit* is used for cases where the

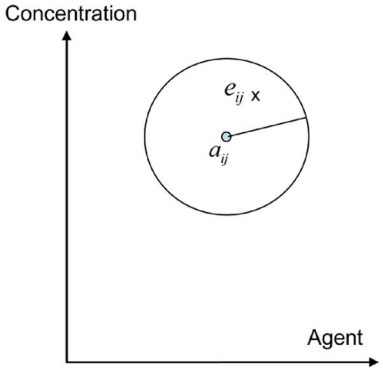

Fig. 3. Actual agent concentration is nonzero. If the estimated concentration is within a small radius of the true concentration, a correct detection is claimed.

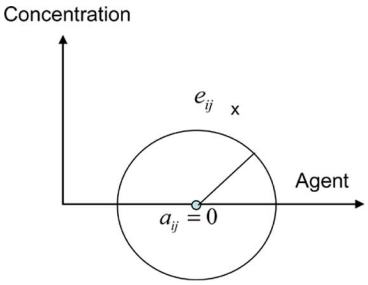

Fig. 4. Actual agent concentration is zero. If the estimated concentration is beyond a small circle, then a false alarm is declared. The circle radius is proportional to a given threshold and threshold varies from 0.001 to some large values. Statistics generated based on each threshold correspond to those points in the ROC curve.

applied detector *correctly* decided that there is "type i gas molecule" in the test measurement). The count for hits is then determined as

$$\text{For } a_{ij} \neq 0 \rightarrow \{\text{if } |e_{ij} - a_{ij}| < (\text{threshold} \times a_{ij})\} \rightarrow h = h + 1. \tag{11}$$

The probability of detection is then computed as

$$\text{PD} = \frac{h}{H} \tag{12}$$

where H is the number of files, where $a_{ij} \neq 0$. The idea is illustrated in Fig. 3. The threshold in (11) is varied to generate different statistics and the final detection rate will be plotted in the ROC curve.

In a similar fashion, suppose f denotes the number of counts for false alarms (it should be noted that the term *false alarm* is used for cases where the applied detector decided that there is type i gas molecule in the test measurement, whereas there is *no* type i gas molecule). The count for false alarms is then determined as

$$\text{For } a_{ij} = 0 \rightarrow \{\text{if } e_{ij} > (\text{threshold} \times 0.5) \rightarrow f = f + 1. \tag{13}$$

The false alarm rate is then computed as

$$\text{FA} = \frac{f}{F} \tag{14}$$

where F is the number of files, where $a_{ij} = 0$.

Fig. 4 illustrates the definition of false alarm.

Different from (11), in (13) it can be seen that "0.5" is used as thebaseline value for actual abundance value. That is, the abundances larger than 0.5 are in advance considered as false alarms and the range to apply ROC curve analysis is thus set to between 0 and 0.5. The ROC curve for gas B molecules is shown

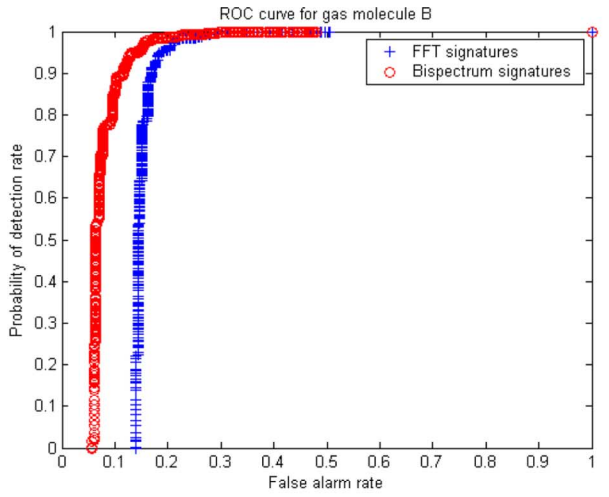

(a)

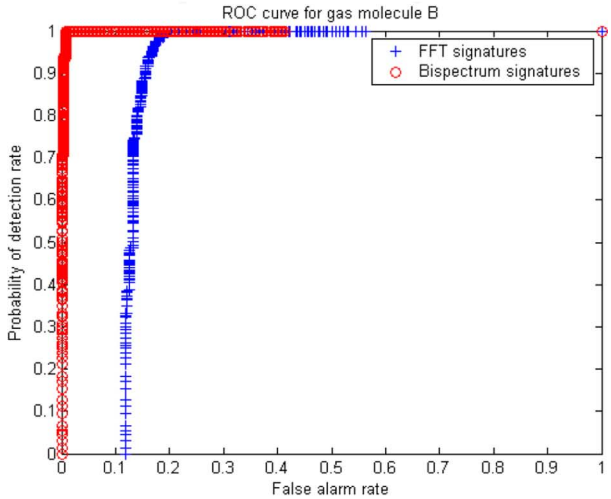

(b)

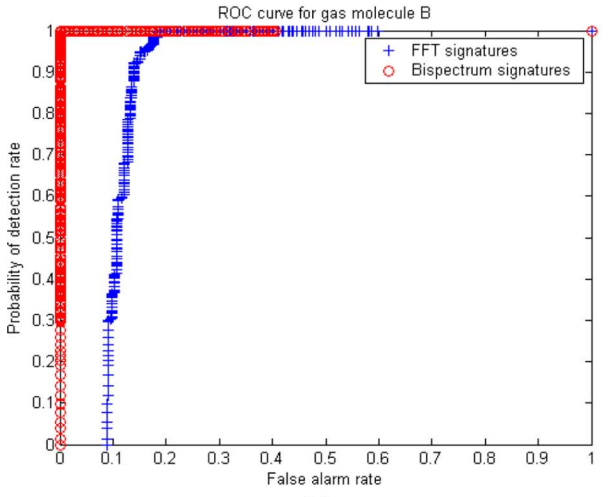

(c)

Fig. 5. ROC curves for gas molecule type B. The more data samples used, the better is the performance of correct classification. (a) Input data: 1 million data points; (b) Input data: 5 million data points; (c) Input data: 10 million data points.

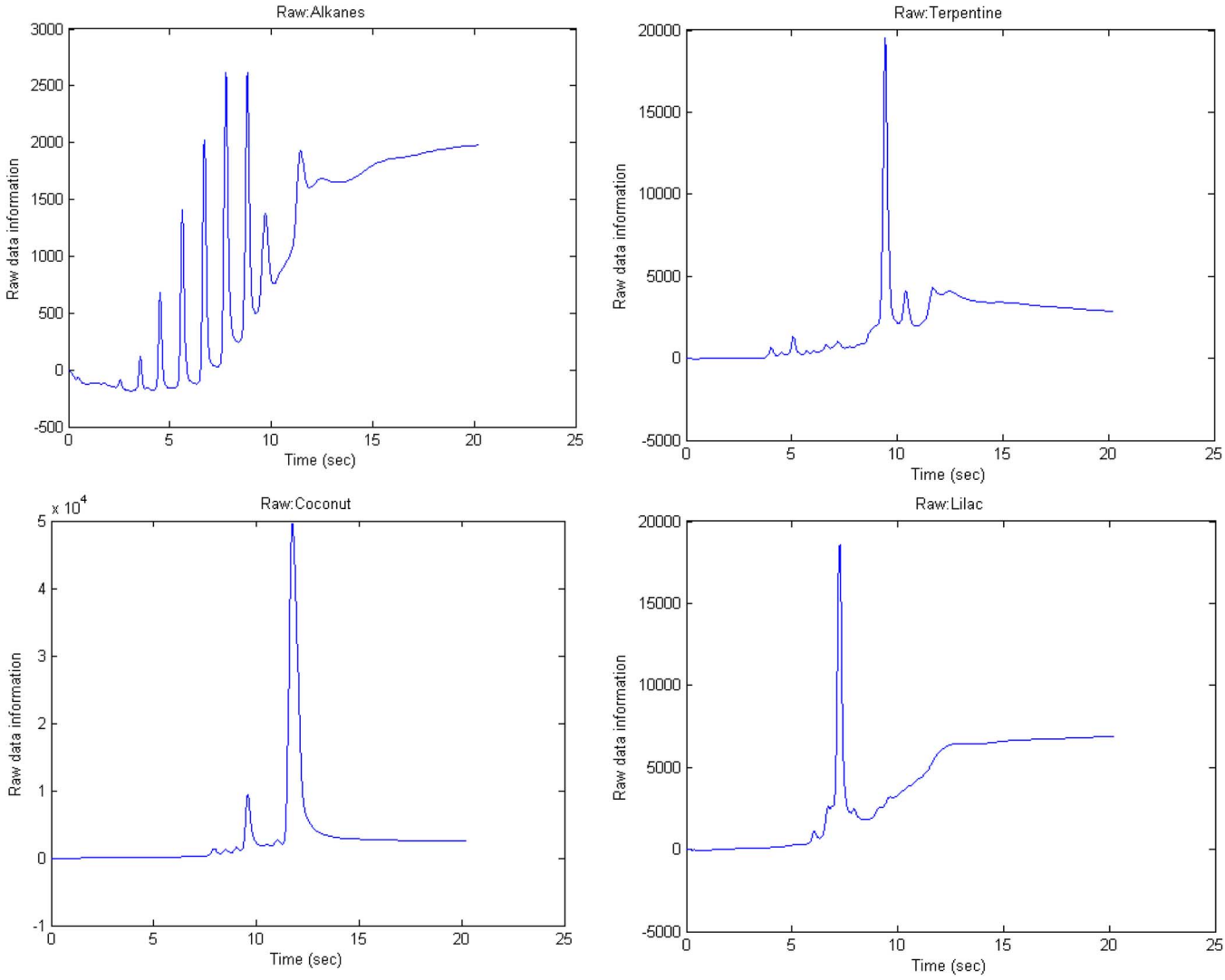

Fig. 6. Raw GC data information of several substances.

in Fig. 5. The ROC curves indicate that bispectrum signatures provided more accurate estimates for gas molecule types B and C, while FFT signatures provided better performance for gas molecule type A. This finding is consistent with the results of the previously applied error-based metric. Moreover, the more data points that we can use in the input, the better the performance (higher probability of detection with less number of false alarms) will be.

In order to compare the concentration estimation performance of the FFT and bispectrum signatures with NCLS, an error metric is defined as follows. Suppose a_{ij} is the actual abundance value of the gas molecule type i for the jth experiment file, where i can be gas molecule type A, B, or C and $j = 1, \ldots, 700$. There are 700 individual files. Suppose e_{ij} is the abundance estimate using the FFT signatures or the bispectrum signatures. Suppose J_i is the error metric for gas molecule type i. The normalized error metric, J_i, can be mathematically expressed as

$$J_i = \frac{\sum_{j=1, a_{ij} \neq 0}^{700} \frac{|a_{ij} - e_{ij}|}{a_{ij}} + \sum_{j=1, a_{ij}=0}^{700} |a_{ij} - e_{ij}|}{700}. \quad (15)$$

TABLE I
ERROR METRIC VALUES FOR THE THREE TYPES OF GAS MOLECULES WITH FFT AND BISPECTRUM SIGNATURES

	Gas A	Gas B	Gas C
FFT signatures	0.052	0.1882	0.2
Bispectrum signatures	0.11	0.13	0.175

In (15), it can be seen that there are two parts in the computation of the error metric. The first part computes the relative error when the actual abundances are *not equal* to zero, and the second part computes the absolute error when the actual abundances are *equal* to zero. From Table I, it can be noticed that with respect to the applied error metric, for gas type molecule A, the FFT signatures provide better performance when compared to the bispectrum signatures, while for the two other gas type molecules B and C, the bispectrum signatures provide more accurate abundance estimates than the FFT signatures provide. The highlighted cells in Table I indicate the lower error metric values which correspond to better performance.

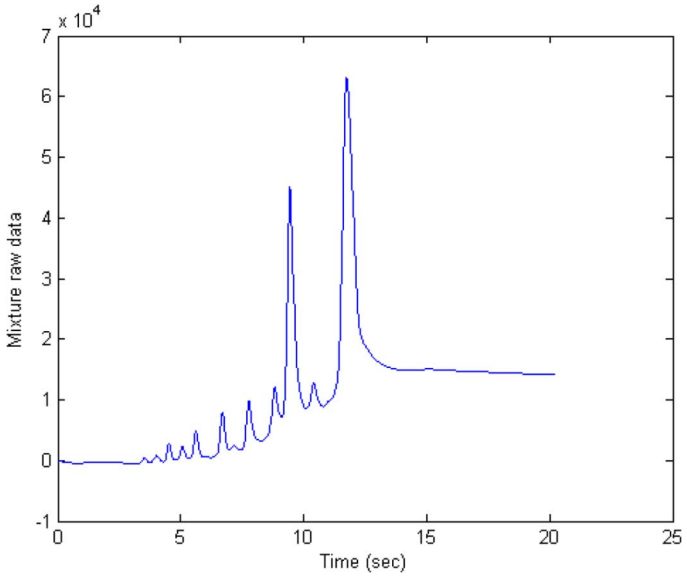

Fig. 7. Raw data of a mixture.

TABLE II
ACTUAL AND ESTIMATED VALUES FOR COMPONENTS IN THE MIXTURE

	Actual	Estimated
Alkanes	3	3.0
Terpentine	2	2.0
Coconut	1	1
Lilac	0	0
Wintergreen	0	0
Smoke	0	0
Paint thinner	0	0
Fruit punch	0	0
Licorice	0	0
Motor oil	0	0.00
Cheddar cheese	0	0

B. Gas Chromatography (GC) Data

The provided GC data from a commercial sensor company correspond to 11 substances. These are: Alkanes, Terpentine, Coconut, Lilac, Wintergreen, Smoke, Paint Thinner, Fruit Punch, Licorice, Motor Oil, and Cheddar Cheese.

There are two data columns for each of the substances. The two data columns are written into an Excel file. The first column corresponds to time. The data collection time is 20.22 s with a sampling time interval of 0.02 s. Thus, there are 1012 samples for each of the substances. The second column corresponds to the first derivative information. There are plots in the Excel files that correspond to the first derivative information with respect to time.

We were given the first derivative information of the 11 substances with respect to time. In Fig. 6, the first derivative information is transformed into raw data information as follows. Suppose $y(n)$ is the first derivative information of the nth sample point, and $x(n)$ is the corresponding raw data information, then the first derivative information of the nth sample point can be expressed as: $y(n) = (x(n+1) - x(n))/\Delta t$, where Δt is the sampling interval. The raw data information for $(n+1)$th sample point can then be computed as $x(n+1) = x(n) + y(n) \times \Delta t$. Since the raw data at time 0 is not provided, it will be assumed that it is equal to 0, $x(0) = 0$.

In this investigation, a signature library is formed using the chromatography signatures of the 11 substances. Instead of the absolute firstt derivative information, the raw data of the 11 substances are included in the signature library. Following that a number of mixtures are *manually* formed with different abundance values of the 11 substances. Our unmixing algorithm is then applied to estimate the individual components in the mixtures. In the following, the formed mixtures, their corresponding *raw* data plots and the estimated coefficients by our method are provided.

Here, we include the results of one study. There are 3 units of Alkanes, 2 units of Terpentine, and 1 unit of Coconut in the mixture. Fig. 7 shows the raw data of mixture. Table II shows the actual and estimated concentration of the three components in the mixtures. The accuracy is very good. In practice, the accuracy may drop due to noise, possible chemical interactions between the components in the mixture, and variations of time arrivals of different components to the detector.

IV. CONCLUSION

In this paper, we present a novel framework for chemical agent detection and concentration estimation. A software product called CAC-CET™ has been designed and implemented by SPI [3]. An Invention Disclosure of the above framework was filed and a patent will be filed soon.

ACKNOWLEDGMENT

The authors would like to thank Dr. D. Woolard, Dr. J. Jensen, and Ms. J. Jensen for their encouragements and valuable inputs during the course of this research.

REFERENCES

[1] C. Kwan, B. Ayhan, G. Chen, C. Chang, J. Wang, and B. Ji, "A novel approach for spectral unmixing, classification, and concentration estimation of chemical and biological agents," *IEEE Trans. Geosci. Remote Sensing*, vol. 44, no. 2, pp. 409–419, Feb. 2006.

[2] E. Osuna, R. Freund, and F. Girosi, "Support vector machines: Training and applications," in *AI Memo 1602*. Cambridge, MA: MIT, 1997.

[3] J. Yin, C. Kwan, F. Chen, D. Dai, T. Yin, T. Puckett, and C. T. Lu, "A flexible and modular software tool for chemical agents classification and concentration estimation," *IEEE J. Sensors*, submitted for publication.

[4] G. Schmera, C. Kwan, P. Ajayan, R. Vajtai, and L. B. Kish, "Fluctuation-Enhanced sensing: Status and perspectives," *IEEE J. Sensors*, submitted for publication.

[5] E. L. Hines, E. Llobet, and J. W. Gardner, "Electronic noses: A Review of signal processing techniques," *IEE Proc. Circuits Devices Syst.*, vol. 146, no. 6, 1999.

[6] M. A. Ryan, H. Zhou, M. G. Buehler, K. S. Manatt, V. S. Mowrey, S. P. Jackson, A. K. Kisor, A. V. Shevade, and M. L. Homer, "Monitoring space shuttle air quality using the jet propulsion laboratory electronic nose," *IEEE Sensors J.*, vol. 4, no. 3, pp. 337–347, 2004.

[7] R. C. Young, W. J. Buttner, R. R. Linnell, and R. Ramesham, "Electronic nose for space program applications," *Sens. Actuators B Chem.*, vol. 93(1-3), pp. 7–16, Aug. 1, 2003.

[8] T. Qian, R. Xu, C. Kwan, B. Linnell, and R. Young, "Toxic vapor classification and concentration estimation for space shuttle and international space station," in *Proc. Int. Symp. Neural Networks*, 2004, pp. 543–561.

[9] T. Qian, X. Li, B. Ayhan, R. Xu, C. Kwan, and T. Griffin, "Application of support vector machines to vapor detection and classification for environmental monitoring of spacecraft," in *Lecture Notes in Computer Science*, J. Wang *et al.*, Ed. New York: Springer, 2006, LNCS 3973, pp. 1216–1222, ISNN 2006.
[10] L. Carmel, N. Sever, D. Lancet, and D. Harel, "An e-nose algorithm for identifying chemicals and determining their concentration," *Sens. Actuators B*, vol. 93, pp. 77–83, 2003.
[11] T. Nishikawa, T. Hayashi, H. Nambo, and H. Kimura, "Feature extraction of multi-gas sensor responses using genetic algorithm," *Sens. Actuators B*, vol. 64, pp. 2–7, 2000.
[12] M. Pardo and G. Sberveglieri, "Classification of electronic nose data with support vector machines," *Sens. Actuators B*, vol. 107, pp. 730–737, 2005.
[13] D. Gao, M. Chen, and J. Yan, "Simultaneous estimation of classes and concentrations of odors by an electronic nose using combinative and modular multilayer perceptrons," *Sens. Actuators B*, vol. 107, pp. 773–781, 2005.
[14] C. D. Natale, A. Macagano, F. Davide, A. D. Amico, A. Legin, Y. Vlasov, A. Rudnitskaya, and B. Selezenev, "Multi-component analysis on polluted waters by means of an electronic tongue," *Sens. Actuators B*, vol. 44, pp. 423–428, 1997.
[15] R. M. Negri and S. Reich, "Identification of pollutant gases and its concentrations with a multisensor array," *Sens. Actuators B*, vol. 75, pp. 172–178, 2001.
[16] L. B. Kish, R. Vajtai, and C.-G. Granqvist, "Extracting information from noise spectra of chemical sensors: Single sensor electronic noses and tongues," *Sens. Actuators B*, vol. 71, pp. 55–59, 2000.
[17] L. B. Kish, R. Vajtai, J. Solis, C. G. Granqvist, and V. Lantto, D. Abbott, V. K. Varadan, and K. F. Boehringer, Eds., "New ways of chemical sensing via fluctuation spectroscopy," in *Proc. SPIE Conf. Smart Electron. MEMS II*, Melbourne, Australia, 2000, vol. 4236.
[18] J. Smulko, C. G. Granqvist, and L. B. Kish, "On the statistical analysis of noise in chemical sensors and its application for sensing," *Fluctuation and Noise Lett.*, vol. 1, pp. 147–153, 2001.
[19] G. Schmera and L. B. Kish, "Surface diffusion enhanced chemical sensing by surface acoustic waves," *Sens. Actuators B*, vol. 93, pp. 159–163, 2003.
[20] J. Smulko, L. B. Kish, and G. Schmera, "Application of nonlinearity measures to chemical sensor signals," *Proc. SPIE Noise and Information in Nanoelectronics Sensors and Standards*, vol. 5115, pp. 92–100, 2003.
[21] G. Schmera and L. B. Kish, "Fluctuation-enhanced gas sensing by surface acoustic wave devices," *Fluctuation and Noise Lett.*, vol. 2, pp. L119–L126, 2002.
[22] G. Shafer, *A Mathematical Theory of Evidence*. Princeton, NJ: Princeton Univ. Press, 1976.

Chiman Kwan (S'85–M'93–SM'98) received the B.S. degree in electronics (Hon.) from the Chinese University of Hong Kong, Hong Kong, in 1988, and the M.S. and Ph.D. degrees in electrical engineering from the University of Texas at Arlington, Arlington, in 1989 and 1993, respectively.

From April 1991 to February 1994, he worked in the Beam Instrumentation Department of the Superconducting Super Collider Laboratory (SSC), Dallas, TX, where he was heavily involved in the modeling, simulation, and design of modern digital controllers and signal processing algorithms for the beam control and synchronization system. He received an invention award for his work at SSC. From March 1994 to June 1995, he joined the Automation and Robotics Research Institute, Fort Worth, TX, where he applied intelligent control methods such as neural networks and fuzzy logic to the control of power systems, robots, and motors. From July 1995 to March 2006, he was with Intelligent Automation, Inc., Rockville, MD. He served as Principal Investigator/Program Manager for more than 65 different projects, with total funding exceeding 20 million dollars. Currently, he is the Chief Technology Officer of Signal Processing, Inc., leading research and development efforts in chemical agent detection, biometrics, speech processing, and fault diagnostics and prognostics. His primary research areas includes fault detection and isolation, robust and adaptive control methods, signal and image processing, communications, neural networks, and pattern recognition applications. He has published more than 50 papers in archival journals and has had 110 additional papers published in major conference proceedings.

Dr. Kwan is a member of Tau Beta Pi. He is listed in the New Millennium edition of *Who's Who in Science and Engineering*.

Gabor Schmera is a Scientist with the Space and Naval Warfare Systems Center, San Diego, CA. His current fields of interest include stochastic and chaotic systems, Monte Carlo simulations, fluctuation-enhanced sensing, and data mining.

Janusz M. Smulko (M'02) was born in Kolno, Poland. He received the M.Sc., Ph.D., and D.Sc. degrees in electronics from the Gdansk University of Technology, Gdansk, Poland, in 1989, 1996, and 2007, respectively. His doctoral research was in $1 = f$ noise measurements in high-frequency bipolar transistors.

Currently, he is with the Faculty of Electronics Telecommunication and Informatics, Gdansk University of Technology, working on problems of low-frequency noise measurements and analysis. In 2003, he joined the Fluctuation and Noise Exploitation Laboratory, Department of Electrical Engineering, Texas A&M University, College Station, as a NATO Postdoctoral Fellow. In 2006, he joined Angström Laboratory, Uppsala University, as a STINT Foundation Research Fellow. His main research activity is concentrated on application of $1 = f$ noise measurements for gas sensing and nondestructive testing.

Laszlo B. Kish is an Interdisciplinary Scientist, working in multiple fields related to stochastic noise/fluctuations in physical, biological, and technological systems. The most known recent results related to his name are probably the Johnson-noise-Kirchhoff-loop secure communicator, the noise and dissipation limits of Moore's law of miniaturization, and fluctuation-enhanced chemical and bacterial sensing. He is the starter and Editor-in-Chief of *Fluctuation and Noise Letters* (World Scientific). He started SPIE's International Symposium Series *Fluctuations and Noise* (2003), and the International Conference Series *Unsolved Problems of Noise* (1996). Currently, he is a Professor at Texas A&M University and before that he had been conducting research in different countries including Hungary (Doctoral Degree, Physics, 1984), Sweden (Docent, Solid-State Physics 1994), The Netherlands, Japan, England, and West Germany.

Dr. Kish was the recipient of the 2001 Benzelius Prize of the Royal Society of Science of Sweden, and the Doctor of Science (Physics) Title of the Hungarian Academy of Science.

Peter Heszler received the M.S. degree in physics in 1983 from the University of Debrecen, Debrecen, Hungary, and the Ph.D. degree in 1988 from the University of Szeged, Szeged, Hungary.

He is a Senior Research Scientist at the University of Szeged. His research interests include FES and chemical agent detection. His research activity has been mostly related to laser-assisted materials science, especially nanoparticle and nanostructure generation by lasers. Recently, his interest turned to the application of nanostructured materials to chemical agent detection by FES, too. He has been conducting research as an Associate Professor and Project Leader in Nanotechnology at Ångstrom Laboratory, Uppsala University, Uppsala, Sweden (Docent, Atomic and Molecular Physics 1994), for several years. Currently, he is a Senior Research Fellow at the Research Group on Laser Physics at the Hungarian Academy of Sciences, University of Szeged, Hungary.

Claes-Göran Granqvist is the Head of the Solid-State Physics Department, Ångström Laboratory, Uppsala University. He was the Vice President for External and International Affairs at Uppsala University, 1997–1999. His interests include optical materials and coatings, nanoparticles, electrochromic materials and devices. He has written, edited, and coedited over 20 books, published over 500 papers, and held over 100 invited talks at international conferences.

Dr. Granqvist is a member of the Royal Swedish Academy of Science. He has received several important awards and prizes, including the Arnberg Prize of the Swedish Royal Academy of Science, the Prize for Best Invention of the Year (Sweden), and the 1998 World Renewable Energy Congress Award.